Environ. Sci. Technol. **1998**, *32*, 1237−1243

A Thermodynamic Approach for Modeling Partitioning of Semivolatile Organic Compounds on Atmospheric Particulate Matter: Humidity Effects

MYOSEON JANG AND
RICHARD M. KAMENS*

Department of Environmental Sciences and Engineering CB# 7400, Rosenau Hall, The University of North Carolina at Chapel Hill, Chapel Hill, North Carolina, 27599

Humidity effects on the gas/particle partitioning of the different types of semivolatile organic compounds (SOCs) in the organic layer of wood soot, diesel soot, and secondary aerosols were studied in outdoor environmental chambers. Experimental partitioning coefficients, K_p, of different SOCs were measured using outdoor Teflon film chambers and compared to theoretical K_p values calculated with the aid of activity coefficients and vapor pressures. A thermodynamic model based on group contribution methods was used to estimate SOC activity coefficients in the liquid organic layer of different atmospheric particles. The equilibrated water content in the organic phase of chemically different particles was estimated from the activity coefficient of water in the particle's organic liquid and the ambient relative humidity (RH). It was found that predicted SOC activity coefficients (${}^i\gamma^\infty_{om}$) for diesel soot particles were not a strong function of RH. There was, however, a dramatic change in ${}^i\gamma^\infty_{om}$ on wood soot particles for hydrophobic compounds such as alkanes and polycyclic aromatic hydrocarbons with changing RH. For polar SOCs, such as *n*-alkanoic acids and substituted phenols on wood soot particles, ${}^i\gamma^\infty_{om}$ did not change with increasing RH. Similar behavior to wood soot particles was observed for ${}^i\gamma^\infty_{om}$ on secondary aerosols from the reaction of α-pinene with O_3. It was concluded that humidity effect on partitioning was most significant for hydrophobic compounds in polar aerosols.

Introduction

Simple relationships for the atmospheric gas/particle (G/P) partitioning of polynuclear aromatic hydrocarbons (PAHs) and other semivolatile organic compounds (SOCs) were presented by Junge (*1*) in 1977 and Yamasaki et al. in 1982 (*2*). Over the past decade, this work has been extended by Pankow, Bidleman, and others (*3*−*10*). There is mounting evidence that G/P partitioning is primarily absorptive in nature and can be described by gas−liquid interaction processes under many conditions (*6*, *11*−*16*). For absorptive partitioning, Pankow (*6*) has shown that the expression for the equilibrium partitioning coefficient, ${}^iK_p$, takes the form of

$$ {}^iK_p = \frac{{}^iC_p}{{}^iC_g \times \mathrm{TSP}} = \frac{7.501RTf_{om}}{10^9 \times \mathrm{MW}_{om}\,{}^i\gamma^\infty_{om}\,{}^ip^\circ_L} \quad (1) $$

where ${}^iC_p$, is the particle-phase concentration, ${}^iC_g$ is the gas-phase concentration, and TSP is the total suspended particulate matter concentration. When ${}^iC_p$ and ${}^iC_g$ have units of nanograms per cubic meter, and TSP has units of micrograms per cubic meter ${}^iK_p$ has units of cubic meters per microgram. The gas constant, R, is 8.314 J $K^{-1}mol^{-1}$. MW_{om} is the average molecular weight of the given organic matter (om), f_{om} is the mass fraction of the absorptive liquidlike material which consists of either organic or inorganic matter (e.g., water) in particles, ${}^i\gamma^\infty_{om}$ is the activity coefficient of an SOC (i) at infinite dilution in a given liquidlike particle medium, and ${}^ip^\circ_L$ is the subcooled liquid vapor pressure of an SOC (i) in torr at a given ambient temperature (T).

If one assumes that ${}^i\gamma^\infty_{om}$ is a constant for nonpolar compounds in a homologous series, the theoretical slope of log ${}^iK_p$ vs log ${}^ip^\circ_L$ should take on a value near −1 (*3*−*8*). However, there are limitations to this assumption, especially when simultaneously treating diverse polar and nonpolar compound classes, and particles with different chemical compositions. This is because SOCs of different compound classes have different activity coefficients in aerosols with different chemical compositions.

Recently, activity coefficient calculation techniques using group contribution methods have been employed for different polarity SOCs in different aerosol liquid layers. This technique provided a dramatic improvement in G/P partitioning predictive capability (*16*). When a new partitioning constant, ${}^iK_{p,\gamma}$, was defined as a product of the measured equilibrium constant, ${}^iK_p$, and ${}^i\gamma^\infty_{om}$ of a given SOC, substantially improved linearity between log ${}^iK_{p,\gamma}$ and log ${}^ip^\circ_L$ was obtained (*16*):

$$ \log({}^i\gamma^\infty_{om}\,{}^iK_p) \equiv \log {}^iK_{p,\gamma} = \log[(7.501RTf_{om})/(10^9 \times \mathrm{MW}_{om})] - \log {}^ip^\circ_L \quad (2) $$

Since ambient humidity can directly influence ${}^i\gamma^\infty_{om}$ and thus the partitioning on different types of particles, this study will focus on thermodynamic model approaches to illustrate the influence of humidity on absorptive G/P partitioning.

Experimental Section

G/P partitioning data for this study were obtained in either 25 or 190 m^3 outdoor Teflon film chambers (*14*, *16*, *17*). All experiments were carried out in the dark to exclude photochemical effects. SOC injections to the gas-phase atmosphere of the chambers were performed in the same manner as described in previous studies (*14*, *16*, *17*). Twenty different SOCs, which include alkanes, alkanoic acids, PAHs, oxygenated and nitrated PAHs, and siloxanes, were used in this study. These compounds are listed in a previous publication (*16*) along with their calculated vapor pressures (*2*−*8*, *18*−*21*).

Combustion particles were added to the chambers after injection of gas-phase SOCs. A 1980 Mercedes Benz 300SD engine was the source of diesel emissions. Wood smoke particles were added to the chamber by burning dry yellow pine in an Arrow catalytic wood stove operated in the catalytic bypass mode. Secondary aerosols from the gas-phase reaction of α-pinene with O_3 were generated in a 190 m^3 outdoor chamber. Two 25 m^3 chambers, designated as east

---

* Corresponding author e-mail: kamens@unc.edu.

S0013-936X(97)00773-6 CCC: $15.00

TABLE 1. Conditions for the Outdoor Smog Chamber Experiments Used for Modeling

date	particle source	chamber[a] (m^3)	*T* (K)	RH (%)	TSP ($\mu g/m^3$)	f_{om}
Oct. 25, 1995	diesel	25 (W)	286–281	83–89	700–270	0.53
Oct. 25, 1995	wood	25 (E)	287–280	76–94	5070–2460	0.98
Aug. 14, 1996	wood	25 (W)	295–291	52–76	3190–1810	0.85
Aug. 14, 1996	wood	25 (E)	296–292	88–93	3900–2130	0.85
Aug. 5, 1996[b]	α-pinene-O_3 reaction	190	296–294	58–64	1420[c]	1.0
Dec. 5, 1996[d]	α-pinene-O_3 reaction	190	271–268	62–92	1390, 1570	1.0

[a] W and E denote the west and east chamber. [b] To generate secondary aerosols, 0.58 ppm ozone was added to 190 m^3 outdoor chamber. [c] TSP for the first sample of the experiment. [d] Secondary aerosols from α-pinene-O_3 reaction used to measure water uptake (*22*).

TABLE 2. Chemical Composition Used for UNIFAC Calculations and Their Activity Coefficients (*16*)

diesel soot composition	^ix	γ_{om}	wood soot composition	^ix	γ_{om}	pinene-O_3 aerosol composition	8/5/96 ^ix	γ_{om}	12/5/96 ^ix	γ_{om}
heneicosane	0.45	1.2	hexadecanoic acid	0.19	4.4	pinic acid	0.87	1.0	0.32	0.9
tetracosane	0.14	1.2	pentanedioic acid	0.07	3.3	2,2-dimethylcyclobutane–1,3-dicarboxylic acid	0.07	0.95	0.04	0.93
hexanoic acid	0.11	1.9	homovanillic acid	0.18	1.9	*cis*-pinonaldehyde	0.06	1.01	0.45	1.03
undecanoic acid	0.17	1.5	4-propyl-benzenediol	0.28	0.9	*cis*-pinonic acid			0.09	0.99
hexadecanoic acid	0.06	1.3	1-guaiacylpropane	0.17	1.2	*cis*-norpinonic acid			0.10	1.01
benzoic acid	0.07	4.9	veratraldehyde	0.11	0.5					
sum	1.00			1.00			1.00		1.00	

and west chambers, were used simultaneously for diesel exhaust and wood smoke experiments on Oct. 25, 1995. These two chambers were also used for a simultaneous dual wood soot experiment (Aug. 14, 1996) to evaluate the effects of different humidity conditions on G/P partitioning. In these types of experiments, the air in one chamber was dried with a standard room dehumidifier, while the air in the other chamber was humidified with a water atomizer. The G/P–phase sampling train consisted of an upstream 40 cm 5-channel annular denuder to collect gas-phase SOCs, a 47 mm Teflon glass fiber filter (type T60A20, Pallflex Products Corp., Putnam, CT) to collect particles and their sorbed SOCs, and another 5-channel denuder to collect particle-phase SOCs released from the particles during sampling (*14, 16, 17*). The detailed sampling and workup procedure and quality control have been reported in other manuscripts (*14, 16, 17, 22*).

Results and Discussion

Activity Coefficient Calculation Techniques. In previously published work (*16*), two methods were used to estimate activity coefficients. In the Hansen's group contribution method (*23–31*), $^i\gamma_{om}^{\infty}$ is calculated from the following expression:

$$RT \ln {}^i\gamma_{om}^{\infty} = {}^iV[({}^{om}\delta_d - {}^i\delta_d)^2 + {}^ib({}^{om}\delta_p - {}^i\delta_p)^2 + {}^ib({}^{om}\delta_h - {}^i\delta_h)^2] + RT\,[\ln({}^iV/V_{om}) + 1 - {}^iV/V_{om}] \quad (3)$$

where ^iV is a molar volume of a compound *i*, V_{om} is the average molar volume of an organic medium in a particle, and δ_d, δ_p, and δ_h are solubility parameters based on dispersion, polar, and hydrogen bonding forces. ^ib is a weighting factor based on dispersional forces (*16, 32*). From compiled molar attraction constants for different functional groups, solubility parameters can be computed (*24, 31*).

The second method called UNIFAC (universal functional group activity coefficient) is commonly used to predict activity coefficients of nonelectrolytes in a liquid medium (*33–37*). UNIFAC has a combinational term ($^i\gamma^C$) that depends on the volume and the surface area of each molecule and a residual term ($^i\gamma^R$) which counts the energetic interaction parameters of different groups based on accumulated experimental data. The relationship between these terms and activity coefficient ($^i\gamma$) is:

$$\ln {}^i\gamma = \ln {}^i\gamma^C + \ln {}^i\gamma^R \quad (4)$$

In this study, the UNIFAC-VLE parameters recently revised by Hansen (*36*) were adopted to calculate activity coefficients at infinite dilution.

Chemically Different Organic Particles. In both the Hansen and UNIFAC techniques, the chemical composition of the sorbant liquid can profoundly influence the activity coefficient of a partitioning SOC (*16*). For this reason, three types of aerosols with different polarities were selected to evaluate humidity effects. Wood smoke particles were used because they are composed of highly oxygenated compounds, such as substituted phenols, substituted aromatic acids, and substituted aromatic aldehydes and ketones (*12, 13, 38–42*). Approximately 70–95% of wood soot aerosols is extractable with organic solvents (*13, 39*). Diesel soot was selected because its organic extract is composed mostly of nonpolar aliphatic hydrocarbons and long-chain aliphatic acids (*43*). The secondary organic aerosol (SOA) formed from the reaction of gas-phase α-pinene with O_3 was used because it produces aldehydes, ketones, and carboxylic acids which are different from those found in either diesel soot or wood soot particles (*44*). This SOA is 100% extractable in polar organic solvents (*16*). In this study, derivatization methods developed by Yu et al. (*45*) and Chien et al. (*46*) were employed to characterize the chemical composition of SOA. Carbonyl products of SOA were derivatized using O-(2,3,4,5,6-pentafluorobenzyl)hydroxylamine hydrochloride (PFBHA) (*45*), and carboxylic acids of these aerosols were identified by pentafluorobenzyl bromide (PFBBr) as a derivatizing agent (*46*). The particle concentrations, temperature, and humidity for the outdoor chamber experiments are shown in Table 1.

Given the general availability of the UNIFAC model, UNIFAC was used in most instances to estimate activity coefficients of SOCs. When interaction parameters were not available in UNIFAC for compounds, such as nitro-PAHs and quinones, the Hansen's group contribution method was used. Table 2 shows the simplified model composition used for UNIFAC calculations with the activity coefficients of the individual components in the three different types of particle liquid layers. Estimated activity coefficients in Table 2 suggest that individual organic compounds associated with a given

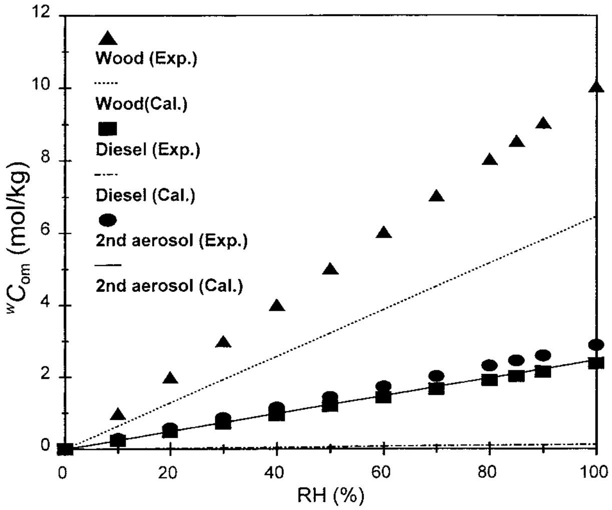

FIGURE 1. Experimental (symbols) and theoretical (lines) water content of different particles (wood smoke particles, diesel soot particles, and α-pinene-O_3 secondary organic aerosols) as a function of %RH.

particle type are most likely miscible with each other under ambient temperatures. These organics, except for organic acids, are immiscible with electrolytic inorganic compounds such as ammonium salts, nitrate, and sulfate, which may constitute 5−40% of the total fine particle matter mass (*47, 48*).

Water Content of Particulate Matter as a Function of Humidity. Water uptake from the gas phase by each atmospheric aerosol varies depending on the nature of the particle chemical composition and its morphology. Vartiainen et al. (*22*) have shown experimentally for wood smoke particles and diesel soot that water uptake is a linear function of RH:

$$\text{water uptake (mg)} = \text{dry particle mass (mg)} \times k_{RH} \times \%RH \quad (5)$$

where the k_{RH} is a proportionality constant for the %RH term. The k_{RH} for wood soot particles was 1.81×10^{-3} and for diesel soot particles was 4.3×10^{-4} over a relative humidity range 45−85% (*22*). In the current study, the experimental water uptake for secondary aerosols from the α-pinene-O_3 reaction was determined by the same procedure (*22*). The k_{RH} for α-pinene-O_3 aerosols was 5.2×10^{-4} over range of 40−70% RH at 24 °C. Dry particle mass of given particulate matter was estimated from the regression intercept of experimental water uptake vs %RH. The moles of water per particle mass, ${}^{w}C_{om,exp}$ (mol/kg), can be calculated by

$${}^{w}C_{om,exp} = 1000k_{RH} \times \%RH/18 \quad (6)$$

From eq 6, it is possible to illustrate the experimental water uptake for wood soot, diesel soot, and α-pinene-O_3 aerosols. This is shown in Figure 1.

A theoretical concentration of water uptake, ${}^{w}C_{om,cal}$, can also be estimated from the vapor pressure of water over an organic medium as described by Raoult's law. For ideal gas behavior, %RH is

$$\%RH = 100\,{}^{w}p/{}^{w}p_L^{\circ} \quad (7)$$

where the ${}^{w}p$ is the partial pressure of water and ${}^{w}p_L^{\circ}$ is the saturated vapor pressure of water. The partial pressure of water is also given by

$${}^{w}p = {}^{w}\gamma_{om}\,{}^{w}x_{om}\,{}^{w}p_L^{\circ} \quad (8)$$

where ${}^{w}\gamma_{om}$ is the activity coefficient of water in the organic matter of a particle, and ${}^{w}x_{om}$ is the mole fraction of water. From the definition of ${}^{w}x_{om}$, eq 7, and eq 8, RH is rewritten by

$$RH = {}^{w}\gamma_{om} n_{H_2O}/(n_{H_2O} + m_o/MW_{om}) \quad (9)$$

where n_{H_2O} is the number of moles of water and m_o is the mass of om in the particle phase. This permits the theoretical water amount (${}^{w}C_{om,cal}$) described by n_{H_2O}/m_o to be computed from MW_{om} and ${}^{w}\gamma_{om}$ in atmospheric particles:

$${}^{w}C_{om,cal}\ (\text{mol/kg}) = RH/MW_{om}/({}^{w}\gamma_{om} - RH) \quad (10)$$

For nonpolar (diesel soot) and moderately polar particles (secondary aerosols), eq 10 can be simplified to

$${}^{w}C_{om,cal}\ (\text{mol/kg}) = \%RH/(100\,{}^{w}\gamma_{om}^{\infty} \times MW_{om}) \quad (11)$$

The theoretical ${}^{w}\gamma_{om}^{\infty}$ is the activity coefficient of water in a dilute condition (Henry's law range), and can also be computed via UNIFAC. It is assumed that ${}^{w}\gamma_{om}^{\infty}$ and MW_{om} in a particle remain unchanged as water is absorbed. This assumption is true only for low water concentrations in the liquid aerosol phase. It may not hold up, however, at high RH in polar media such as wood soot if the amount of absorbed water is above the range of Henry's law. For wood soot, the activity coefficient (${}^{w}\gamma_{om}$) becomes a function of the RH or water content in particulate matter. The ${}^{w}\gamma_{om}$ in UNIFAC calculation for wood soot increases as a function of water uptake.

Figure 1 also compares the predicted ${}^{w}C_{om,cal}$ using UNIFAC with the measured water uptake by eq 6. MW_{om} was calculated from the model chemical composition of each aerosol medium. For wood soot particles, the ${}^{w}\gamma_{wood}^{\infty}$ by UNIFAC gave a value of ∼1. This implies that absorbed water in wood soot particles is homogeneously miscible with the organic medium of these hydrophilic particles. As shown in Figure 1, ${}^{w}C_{om,cal}$ calculated from ${}^{w}\gamma_{wood}^{\infty}$ only for the organic portion of the particle was compared to ${}^{w}C_{om,exp}$. Because the predicted water content is overestimated and deviates from Henry's law range as increasing humidity, ${}^{w}C_{om,cal}$ is extrapolated by regression using low humidity range of ${}^{w}C_{om,cal}$ values which are within the Henry's law range. ${}^{w}C_{om,cal}$ was consistently lower (∼35%) than the observed ${}^{w}C_{wood,exp}$. Wood smoke particles, however, contain inorganic metals and salts, organic polymers, and surfactants (*47, 48*). One explanation for differences between ${}^{w}C_{wood,exp}$ and ${}^{w}C_{wood,cal}$ is the contribution of hygroscopic inorganic salts (such as sodium, potassium, chlorides, nitrates, ammonium, and sulfates) to the overall water content for wood smoke particles.

Aerosols from the reaction of α-pinene with O_3 in the outdoor chamber do not include hygroscopic salts because they are formed solely from just condensed organics. Thus, ${}^{w}C_{\alpha\text{-p,cal}}$ agrees well with ${}^{w}C_{\alpha\text{-p,exp}}$ at 98% confidence level and has a standard error of 16% (Figure 1). The UNIFAC-calculated water activity coefficient of α-pinene-O_3 aerosols (${}^{w}\gamma_{\alpha\text{-p,cal}}^{\infty}$) on Dec. 5, 1996 was 2.4. This indicates that water has less preference for secondary aerosols than for wood-soot particles. Based on ${}^{w}\gamma_{\alpha\text{-p,cal}}^{\infty}$, a maximum solubility of ∼0.4 mole fraction units was estimated. When the %RH was 99% at 25 °C, the modeled water uptake estimated by eq 11 was 0.29 in mole fraction units (2.47 mol/kg of particulate matter or 3.9 wt % of organic matter). This still is lower than the saturated water content as calculated from UNIFAC and suggests that the water content of α-pinene-O_3 aerosols under ambient conditions is less than its saturation solubility. Such

TABLE 3. Fitting Coefficients,[a] *a* and *c*, for Wood Soot Particles and α-pinene-O$_3$ Aerosols[b]

compounds	2nd aerosol *a*	2nd aerosol *c* (×10^5)	wood soot *a*	wood soot *c* (×10^5)
fluorene	934	591	453	805
phenanthrene	989	643	500	878
pyrene	1505	745	711	1030
benz[*a*]anthracene	1723	836	755	1160
9-methylanthracene	1179	681	373	1110
heptadecane	11 975	624	4964	722
nonadecane	17 724	701	6665	822
eicosane	21 478	740	7692	876
docosane	31 359	816	10 194	975
dodecanoic acid	514	61	491	−263
tetradecanoic acid	707	138	610	−162
hexadecanoic acid	972	214	759	−62
9,10-anthraquinone	609	131	476	307
9-nitroanthracene	555	191	460	239
phenanthrene−9-carboxaldehyde	877	464	317	633
4-biphenylcarboxaldehyde	642	361	249	477
BHT	397	−700	147	−710
3,5-dimethylphenol	239	−770	127	−1000
2-isopropylphenol	313	−766	161	−410
decamethylcyclosiloxane	1008	−820	11 779	−996
hydroxynonamethylcyclosiloxane	2137	−431	4344	−1540

[a] *a* and *c* were numerically determined by fitting $^i\gamma^\infty_{\mathrm{om}} \times \mathrm{MW_{om}}$ to the form $a\exp^{c \times \%\mathrm{RH}}$. [b] Fitting parameters of α-Pinene-O$_3$ secondary aerosols were calculated from the composition of 8/5/1996 samples.

estimations are unnecessary for wood soot particles given the very high solubility of water in the organic layer of these particles.

From UNIFAC, the theoretically calculated water activity coefficient for diesel soot, $^w\gamma^\infty_{\mathrm{diesel}}$ was 32, reflecting that organic components in diesel soot particles are extremely hydrophobic. At significant water absorption beyond the saturation point, a phase separation between water and the organic layer of diesel soot would occur. Figure 1 shows that the theoretically calculated $^wC_{\mathrm{diesel,cal}}$ is much lower than the experimentally determined $^wC_{\mathrm{diesel,exp}}$. Although the hygroscopic inorganic salt content is only 1−2% of wood or diesel combustion particles, it appears to contribute significantly to water uptake of these aerosols. Given the hydrophobic nature of organics in diesel soot particles, the disparity between the theoretical and experimental results suggests that the overall water content of diesel soot is more strongly influenced by hydrophilic inorganics than in wood soot particles.

The uniform water uptake of inorganic salts in atmospheric aerosols has been studied by Pilinis et al. (*49*) and Kim et al. (*50*). As humidity increases, it is also possible that the water absorbed by organic−inorganic atmospheric particles may form small islands or clusters around inorganic sites (*21*). These clusters would be formed separately from the organic layer of the particles. From a G/P-partitioning perspective, most of the SOC absorption will take place in the organic liquid portion of the particle. If an inorganic-water zone exists, partitioning of SOCs into this matrix will be of little importance given the very high activity coefficients and low solubilities in such a liquid phase for most SOCs except highly polar water-soluble organics.

Humidity vs Partitioning. The water concentration of the aerosol can be computed as a function of %RH (eq 11). This permits a reconstruction of the entire chemical composition of the aerosol as a function of %RH. This new composition including water can then be used to recalculate $^i\gamma^\infty_{\mathrm{om}}$ as a function of %RH for different aerosol liquid layers. For diesel soot particles (Graph 1 in Supporting Information), the predicted $^i\gamma^\infty_{\mathrm{om}}$ of SOCs does not change significantly as a function of %RH. In wood soot particles, however, the $^i\gamma^\infty_{\mathrm{om}}$ of hydrophobic compounds such as alkanes and PAHs

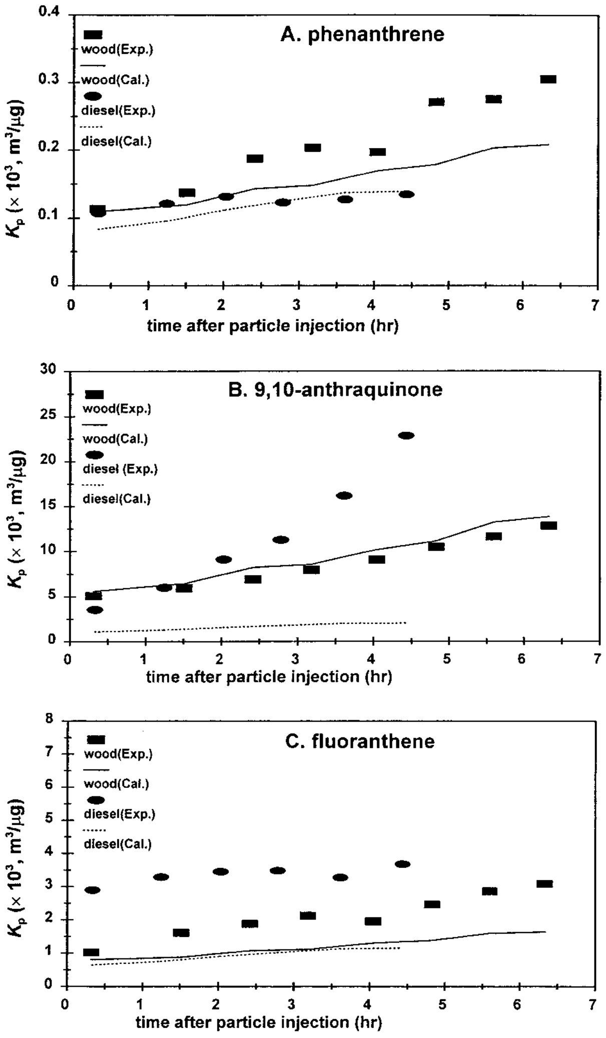

FIGURE 2. K_p values for selected SOCs in dual chamber experiments using wood soot and diesel soot on Oct. 25, 1995.

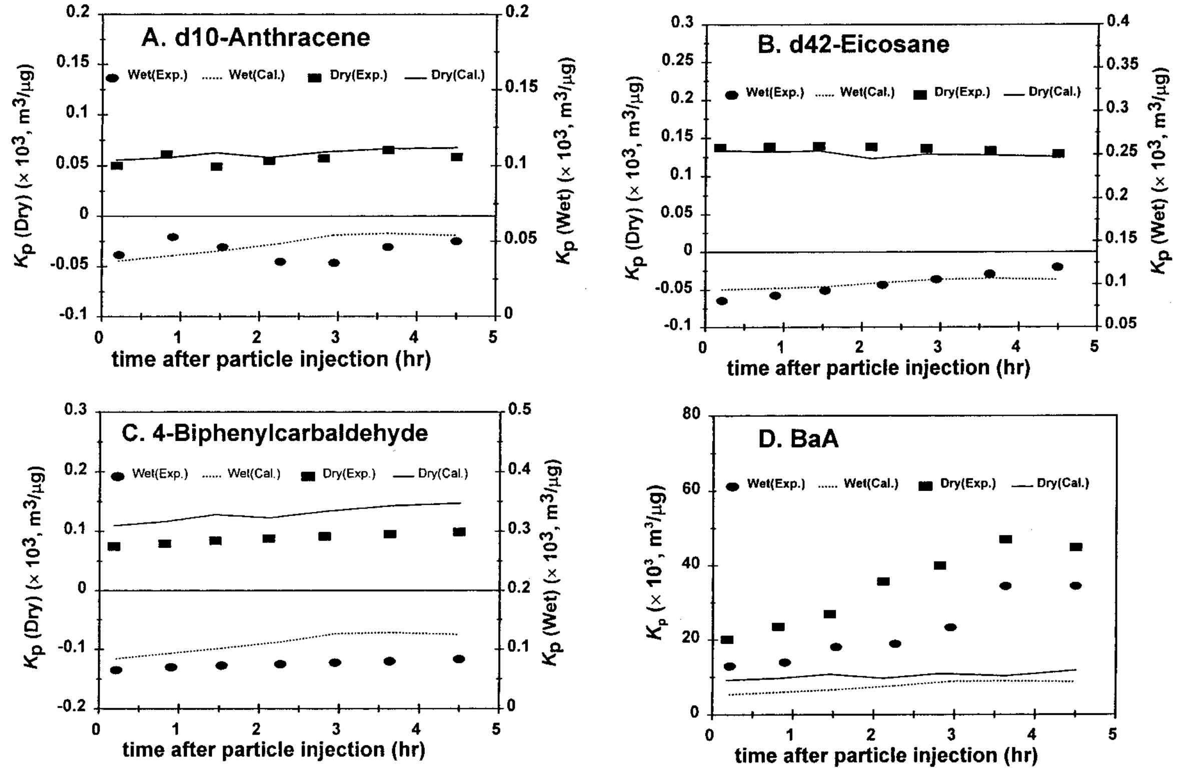

FIGURE 3. Experimental and calculated K_p values for wood smoke particles in dual outdoor chamber experiments under different relative humidities on Aug. 14, 1996.

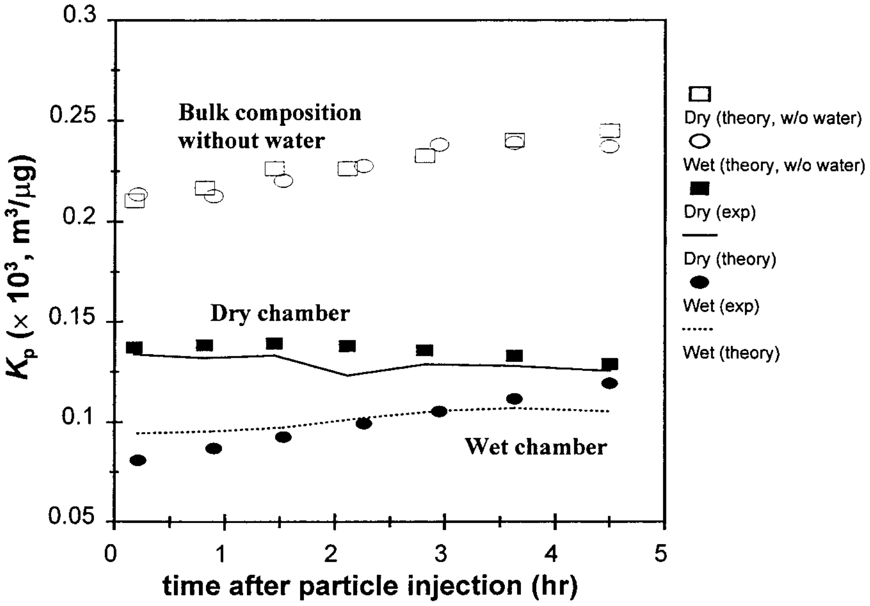

FIGURE 4. Experimental and theoretical K_p values of d_{42}-eicosane for two differently controlled RH conditions using two outdoor chambers with the same wood smoke particles on Aug. 14, 1996.

increases with increasing %RH (Graph 2 in Supporting Information). This means that the solubility of hydrophobic SOCs in the aerosol phase decreases with increasing RH. As expected with wood smoke particles, ${}^i\gamma_{om}^{\infty}$ for polar compounds such as phenols (e.g., BHT) and alkanoic acids (e.g., tetradecanoic acid) does not change significantly with RH compared to nonpolar SOCs (e.g., eicosane and BaA). Similar behavior for ${}^i\gamma_{om}^{\infty}$ was observed for the α-pinene-O_3 aerosols (Graph 3 in Supporting Information).

For a given particulate organic composition, ${}^i\gamma_{om}^{\infty}$ and MW_{om} are functions of %RH and can be related to %RH by fitting to the form, $a \exp^{c \times \%RH}$, where a and c are fitting parameters. Substituting $a \exp^{c \times \%RH}$ for ${}^i\gamma_{om}^{\infty} \times MW_{om}$ in eq 1 gives an expression for log ${}^iK_p$ as a function of %RH:

$$\log {}^iK_p = \text{int} - (0.434c \times \%RH) - \log {}^ip_L^{\circ} \qquad (12)$$

where the intercept, int, equals $\log [7.501 f_{om} RT/(10^9 a)]$. The fitting parameter c indicates the sensitivity of log ${}^iK_p$ as a function of %RH. The calculated fitting parameters of SOCs are listed in Table 3. Since %RH is easily obtained for most systems, %RH in eq 12 can be employed as a surrogate for the activity coefficient. The relationship between %RH vs log ${}^iK_p$ can then be used to illustrate how ${}^iK_p$ changes with ambient temperature and humidity in our outdoor chambers. This is illustrated for a dual-chamber outdoor experiment (Oct. 25, 1995) in our 25 m^3 chambers with wood soot in one chamber and diesel combustion exhaust in the other. The temperature and %RH conditions for this experiment are shown in Table 1. In Figure 2, experimental ^iK_p values of several SOCs are compared with the theoretical ^iK_p values estimated from the experimental temperature, humidity, and compositional effects of the different exhaust particles. For wood smoke particles, phenanthrene (Figure 2A), and 9,-10-anthraquinone (Figure 2B) show reasonable agreement between experimental and theoretical ^iK_p values. For these same particles, the theoretically predicted ^iK_p value for fluoranthene (Figure 2C) was initially close to the experimental ^iK_p value. As the system aged over 6 h, however, the experimental and theoretical ^iK_p values of fluoranthene diverged by a factor of 2, whereas phenanthrene illustrated somewhat less difference (about 25%). Adsorption of the analytes to the elemental carbon core of the particles may be responsible for this process.

For the diesel exhaust system, the predicted ^iK_p values of phenanthrene (like wood smoke system) also provided good agreement with experimental ^iK_p values as shown in Figure 2A. However, theoretically estimated ^iK_p values for 9,10-anthraquinone (Figure 2B) and fluoranthene (Figure 2C) on diesel soot deviated significantly from their corresponding experimental ^iK_p values. As with fluoranthene on wood soot particles, adsorption to carbon core material in diesel soot particles may occur to a significant extent for high molecular weight PAHs and substituted PAHs. In addition, the compounds may be deviating from G/P-partitioning equilibrium due to transport impedances in the particles. As such, particles may not be able to offgas SOCs rapidly enough in response to gas-phase concentration changes (adsorption to chamber walls) to maintain G/P-partitioning equilibrium (*51, 52*).

To further illustrate humidity effects on G/P partitioning of SOCs, another dual outdoor chamber experiment (Aug. 14, 1996) was carried out with different %RHs in each chamber (Table 1). The %RH of the “dry” chamber ranged from 52 to 76%, and the “wet” chamber ranged from 88 to 93%. The model predictions of ^iK_p values of several SOCs are compared to experimental ^iK_p values in Figure 3. Both the experimental and theoretical results showed that partitioning of SOCs to “dry” particles was higher than that to “wet” particles. This is consistent with the observation of Pankow et al. (*53*) for urban aerosols in Osaka, Japan. In the case of d_{10}-anthracene (Figure 3A), d_{42}-eicosane (Figure 3B), and 4-biphenylcarbaldehyde (Figure 3C), predicted and experimental ^iK_p values compare well with each other. However, poor comparisons of ^iK_p for benz[*a*]anthracene (high MW PAH, Figure 3D) were observed. This poor agreement was most probably due to strong adsorption onto the particle core which is more significant for high molecular weight SOCs.

As a last example, the predicted ^iK_p values and their experimental ^iK_p values for d_{42}-eicosane are displayed in Figure 4, and compared to predicted ^iK_p values using the composition of wood smoke excluding water. The difference between ^iK_p values in two chamber experiments with different RHs can be explained by the activity coefficients at different humidities. When water was excluded from the ^iK_p activity coefficient calculation, it was not possible to closely simulate experimentally observed ^iK_p values. Hence, an important observation is that G/P-partitioning estimations of hydrophobic SOCs on polar or semipolar organic aerosols are significantly influenced by humidity effects. For less polar aerosols such as diesel soot particles, humidity effect on partitioning of SOCs is not as important.

Acknowledgments

This work was supported by a Grant from the National Science Foundation to the University of North Carolina (ATM 9708533, Dr. Sherry O. Farwell, Project Officer). The authors would like to thank Michael Strommen and Keri Leach for assisting with chamber experiments.

Supporting Information Available

Three figures (3 pages) will appear following these pages in the microfilm edition of this volume of the journal. Photocopies of the Supporting Information from this paper or microfiche (105 × 148 mm, 24x reduction, negatives) may be obtained from Microforms Office, American Chemical Society, 1155 16th St. NW, Washington, DC 20036. Full bibliographic citation (journal, title of article, names of authors, inclusive pagination, volume number, and issue number) and prepayment, check or money order for $12.00 for photocopy ($14.00 foreign) or $12.00 for microfiche ($13.00 foreign), are required. Canadian residents should add 7% GST. Supporting Information is also available via the World Wide Web at URL http://www.chemcenter.org. Users should select Electronic Publications and then Environmental Science and Technology under Electronic Editions. Detailed instructions for using this service, along with a description of the file formats, are available at this site. To download the Supporting Information, enter the journal subscription number from your mailing label. For additional information on electronic access, send electronic mail to si-help@acs.org or phone (202) 872-6333.

Glossary

a	coefficient to fit ($^i\gamma^\infty_{om}$ × MW_{om}) to $a\exp^{c \times \%RH}$
^ib	weighting factor
BHT	2,6-di-*tert*-butyl-4-methylphenol
c	coefficient to fit ($^i\gamma^\infty_{om}$ × MW_{om}) to $a\exp^{c \times \%RH}$
^iC_g	gas-phase concentration of a compound (i) (ng/m^3)
$^wC_{om}$	concentration of water in om phase of a particle (mol/kg)
$^wC_{om,exp}$	experimentally calculated water concentration in a given om (diesel soot, wood soot, and α-p) of a particle (mol/kg)
$^wC_{om,cal}$	theoretically calculated water concentration in a given om (diesel soot, wood smoke, and α-p) of a particle (mol/kg)
^iC_p	particle phase concentration of a compound (i) (ng/m^3)
d	denotation for a dispersion term
$D_4D'OH$	hydroxynonamethylcyclosiloxane
D_5	decamethylcyclosiloxane
f_{om}	the mass fraction of the absorptive liquidlike material
h	denotation for a hydrogen-bonding term
int	theoretical intercept of log ^iK_p vs log p°_L and %RH log[$7.501 f_{om}RT/(10^9 a)$]
k	functional group in an organic molecule
k_{RH}	regression slope for water uptake vs %RH
^iK_p	gas/particle partitioning coefficient for a compound (i)
$^iK_{p,\gamma}$	activity coefficient adjusted partitioning coefficient, $^iK_{p,\gamma} \equiv {}^i\gamma_{om}{}^iK_p$
m_o	mass of *om* in the particle phase

$n_{\mathrm{H_2O}}$	number of moles of water
$\mathrm{MW_{om}}$	average molecular weight of a given om
om	organic medium of a particle
p	denotation for a polar term
^{w}p	partial pressure (mm Hg) of water
PAH	polynuclear aromatic hydrocarbon
$^{i}p_{\mathrm{L}}^{\circ}$	sub-cooled liquid vapor pressure (Torr) of a compound (i)
R	gas constant (8.314 J K^{-1} mol^{-1})
RH	relative humidity
SOA	secondary organic aerosol
SOC	semivolatile organic compound
T	temperature (K)
TSP	total suspended particulate matter (μg/m^3)
UNIFAC	universal functional group activity coefficient
^{i}V	molar volume of a SOC (i)
VLE	vapor-liquid equilibrium
V_{om}	average molar volume of a given om in a particle
^{i}x	mole fraction of a component (i)
$^{w}x_{\mathrm{om}}$	mole fraction of a water in a given om
α-p	α-pinene-$\mathrm{O_3}$ secondary aerosols
$^{w}\gamma_{\mathrm{om}}$	activity coefficient of water in a given om
$^{i}\gamma_{\mathrm{om}}^{\infty}$	diluted activity coefficient of an organic compound (i) in a given om
$^{i}\gamma^{\mathrm{C}}$	combinational term for an activity coefficient in UNIFAC
$^{i}\gamma^{\mathrm{R}}$	residual term for an activity coefficient in UNIFAC
$^{i}\delta$	solubility parameter of a compound (i)
$^{om}\delta$	solubility parameter of om

Literature Cited

(1) Junge, C. E. In *Fate of Pollutants in the Air and Water Environ.*; Suffet, I. H., Ed.; Wiley-Interscience: New York, 1977; pp 7−25.

(2) Yamasaki, H.; Kuwata, K.; Miyamoto, H. *Environ. Sci. Technol.* **1982**, *16*, 189−194.

(3) Pankow, J. F. *Atmos. Environ.* **1987**, *21*, 2275−2283.

(4) Pankow, J. F. *Atmos. Environ.* **1991**, *25*A, 2229−2239.

(5) Pankow, J. F.; Bidleman T. F. *Atmos. Environ.* **1992**, *26*A, 1071−1080.

(6) Pankow, J. F. *Atmos. Environ.* **1994**, *28*, 185−188.

(7) Pankow, J. F.; Isabelle, L. M.; Bucholz, D. A.; Luo, W.; Reeves, B. D. *Environ. Sci. Technol.* **1994**, *28*, 363−365.

(8) Story, J. M. E.; Luo, W.; Isabelle, L. M.; Pankow, J. F. *Environ. Sci. Technol.* **1995**, *29*, 2420−2428.

(9) Bidleman, T. F.; Billings, W. N.; Foreman, W. T. *Environ. Sci. Technol.* **1986**, *20*, 1038−1043.

(10) Finizio, A.; Mackay, D.; Bidleman, T.; Harner, T. *Atmos. Environ.* **1997**, *31*, 2289−2296.

(11) Ross, M.; Risby, T. H.; Steel, W. A.; Yasbin, R. E. *Colloids Surf.* **1982**, *5*, 17−31.

(12) McDow, S. R.; Sun Q.; Vartiainen, M.; Hong Y.; Yao Y.; *Environ. Sci. Technol.* **1994**, *28*, 2147−2153.

(13) McDow, S. R.; Jang, M.; Hong, Y.; Kamens, R. M. *J. Geophys. Res.* **1996**, *101*, 19593−19600.

(14) Kamens, R. M.; Odum, J. R.; Fan, Z. *Environ. Sci. Technol.* **1995**, *29*, 43−50.

(15) Liang, C.; Pankow, J. F.; Odum, J. R.; Seinfeld, J. H. *Environ. Sci. Technol.* **1997**, *31*, 3086−3092.

(16) Jang, M.; Kamens, R. M.; Leach, B. K.; Strommen, M. R. *Environ. Sci. Technol.* **1997**, *31*, 2805−2811.

(17) Fan, Z.; Kamens, R. M.; Hu, J.; Zhang, J. *Environ. Sci. Technol.* **1996**, *30*, 1359−1364.

(18) Yamasaki, H. K.; Kuge, Y. *Nippon Kagaku Kaishi* **1984**, *8*, 1324−1329.

(19) Tao, Y.; McMurry, P. H. *Environ. Sci. Technol.* **1989**, *23*, 1519−1523.

(20) Reid, R. C.; Prausnitz, J. M.; Poling, B. E. *The Properties of Gases and Liquids*, 4th ed.; McGraw-Hill: New York, 1987.

(21) Schwarzenbach, R. P.; Gschwend, P. M.; Imboden, D. M. *Environmental Organic Chemistry*; John Wiley & Sons: New York, 1993.

(22) Vartiainen, M.; McDow, S. R.; Kamens, R. M. *Chemosphere* **1994**, *29*, 1661−1669.

(23) Meusburger, K. E. *Am. Chem. Soc. Symp. Ser.* **1988**, *371*, 151−162.

(24) Barton, A. F. M. *CRC Handbook of Solubility Parameters and Other Cohesion Parameters*, 2nd ed.; CRC Press: Boston, 1991.

(25) Hildebrand, J. H.; Scott, R. L. *Solubility of Non-Electrolytes*, 3rd ed.; Reinhold Publishing: New York, 1950.

(26) Hildebrand, J. H.; Scott, R. L. *Regular Solutions*; Prentice Hall: Englewood Cliffs, NJ, 1962.

(27) Barton, A. F. M. *Chem. Rev.* **1975**, *75*, 731−753.

(28) Hansen, C. M. *J. Paint Technol.* **1969**, *39*, 104−117.

(29) Bicerano, J. *Prediction of Polymer Properties*; Marcel Dekker: New York, 1993.

(30) Hansen, C. M.; Andersen, B. H. *Am. Ind. Hyg. Assoc. J.* **1988**, *49*, 301−308.

(31) Van Krevlen, D. W. *Properties of Polymers: Their Correlation with Chemical Structure; Their Numerical Estimation and Prediction from Additive Group Contributions*, 3rd ed.; Elsevier Science Publisher: New York, 1990.

(32) Lo, T. C.; Baird, M. H. I.; Hanson, C. *Handbook of Solvent Extraction*; John Wiley & Sons: New York, 1983.

(33) Sandler, S. I. *Chemical and Engineering Thermodynamics*; John Wiley & Sons: New York, 1989.

(34) Fredenslund, A.; Sorensen, J. M. In *Models for Thermodynamic and Phase Equilibria Calculations*; Heinemann, H. Ed.; Marcel Dekker: New York, 1994.

(35) Gmehling, J.; Rasmussen, P.; Fredenslung, A. *Ind. Eng. Chem. Res.* **1982**, *21*, 118−127.

(36) Hansen, H. K.; Rasmussen, P. *Ind. Eng. Chem. Res.* **1991**, *30*, 2352−2356.

(37) Fredenslung, A.; Jones, R. M.; Prausnitz, J. M. *AIChE J.* **1975**, *21*, 1086.

(38) Rogge, W. F. In *Determination of Key Organic Compounds Present in the Particulate Matter Emissions from Air Pollution Sources*, final report to EPA, CA., 1993, contract No. 8932-127.

(39) Kamens, R. M.; Guo, Z.; Fulcher, J. N.; Bell, D. A. *Environ. Sci. Technol.* **1988**, *22*, 103−108.

(40) Jang, M.; McDow, S. R. *Environ. Sci. Technol.* **1995**, *29*, 2654−2660.

(41) Jang, M.; McDow, S. R. *Environ. Sci. Technol.* **1997**, *31*, 1046−1053.

(42) Odum, J. R.; McDow, S. R.; Kamens, R. M. *Environ. Sci. Technol.* **1994**, *28*, 1285−1290.

(43) Rogge, W. F.; Hildemann, L. M.; Mazurek, M. A.; Cass, G. R. *Environ. Sci. Technol.* **1993**, *27*, 636−651.

(44) Hull, L. A., In *Atmospheric Biogenic Hydrocarbons*; Bufalini, J. J.; Arnts, R. R., Ed.; Butterworth: Stoneham, 1981, Vol. 2, pp 161−186.

(45) Yu, J.; Jeffries, H. E.; Le Lacheur, R. M. *Environ. Sci. Technol.* **1995**, *29*, 1923−1932.

(46) Chien, C.; Charles, M. J.; Sexton, K. G.; Jeffries, H. E. *Environ. Sci. Technol.* **1998**, *32*, 299−309.

(47) Rogge, W. F.; Mazurek, M. A.; Hildemann, L. M.; Cass, G. R. *Atmos. Environ.* **1993**, *27*A, 1309−1330.

(48) Hildemann, L. M.; Markowski, G. R.; Cass, G. R. *Environ. Sci. Technol.* **1991**, *25*, 744−795.

(49) Pilinis, C.; Seinfeld, J. H. *Atmos. Environ.* **1989**, *23*, 1601−1606.

(50) Kim, Y. P.; Seinfeld, J. H. *Aerosol Sci. Technol.* **1993**, *19*, 157−181.

(51) Odum, J. R.; Yu, J.; Kamens, R. M. *Environ. Sci. Technol.* **1994**, *28*, 2278−2285.

(52) Strommen, M. R.; Kamens, R. M. *Environ. Sci. Technol.* **1997**, *31*, 2983−2990.

(53) Pankow, J. F.; Storey, J. M. E.; Yamasaki, H. *Environ. Sci. Technol.* **1994**, *27*, 2220−2226.

Received for review August 29, 1997. Revised manuscript received January 21, 1998. Accepted January 27, 1998.

ES970773W